厚生労働科学研究費補助金

厚生労働省臨床研究基盤整備推進研究事業

局所限局非小細胞肺がんの集学的治療に関する研究

平成18年度　総括研究報告書

主任研究者　加藤　治文

平成19（2007）年4月

目　次

厚生労働科学研究費補助金(がん臨床研究事業)

総括研究報告書

局所限局非小細胞肺がんの集学的治療に関する研究

主任研究者　加藤治文　東京医科大学病院外科学第一講座教授

研究要旨：本年度の研究では、プラチナ製剤を含む2剤併用療法のレジメンとして、本邦で最も汎用されているという理由からカルボプラチンとパクリタキセル(CP 療法)の認容性、安全性に関わる臨床第Ⅱ相試験を個別研究として行う一方で、臨床第Ⅲ相試験のデザインと実施計画書の作成を検討した。当初計画した本臨床第Ⅲ相試験の対象は、完全切除された病理病期ⅠB-ⅢA 期非小細胞肺癌例としていた。しかし、2006年6月の米国臨床腫瘍学会(ASCO)において、シスプラチンを含む2剤併用療法による術後化学療法のメタアナリシス:Lung Adjuvant Cisplatin Evaluation(LACE)の結果と対象を臨床病期IB期に特化したCALGB9633の追加報告がなされ、病期によっては化学療法のリスクがベネフィットを上回る可能性が示唆され、術後化学療法によってIA期ではむしろ死亡リスクが高くなり、ⅠB期では生存の延長に寄与することに疑問を残す結果であった。以上の経緯を踏まえグループ内で議論した結果、対象集団をプラチナ製剤の有効性が示されたII、III期と本邦においてのみ有効性が示されたIB期に分けて、新たに大規模臨床試験を計画する方針とした。IB期においてはUFT投与群を対照として経口抗がん剤であるテガフール・ギメラシル・オテラシルカリウム配合剤(S-1)の有用性を評価する試験を、II-IIIA 期に対しては、プラチナ製剤を含む 2 剤併用療法投与群を対照として経口剤もしくは分子標的薬剤の維持療法としての上乗せ効果を検証する試験をそれぞれ検討中である。

分担研究者;
一瀬幸人(国立病院九州がんセンター腫瘍外科部長)、岡田守人(兵庫県立成人病センター呼吸器外科科長)、國頭英夫(国立がんセンター中央　総合病棟部)、小池輝明(新潟県立がんセンター新潟病院腫瘍外科部長)、近藤丘(東北大学加齢医学研究所呼吸器外科教授)、鈴木健司(国立がんセンター中央病院呼吸器外科医員)、多田弘人(大阪市立総合医療センター呼吸器外科部長)、坪井正博(東京医科大学病院外科学第一講座講師)、太田三徳(大阪府立呼吸器・アレルギー医療センター、呼吸器外科部長)、光冨徹哉(愛知県がんセンター腫瘍外科部長)、吉田純司(国立がんセンター東病院呼吸器外科医長)、山本信之(静岡県立静岡がんセンター呼吸器内科部長)

A.　研究目的:

1)奏効率・毒性の異なる二種類の化学療法レジメンから術前・術後化学療法への適性を検討し、臨床第Ⅲ試験の試験治療を決定する。

2)臨床病期(c-Stage)IB-II 非小細胞肺癌(NSCLC)に対する術後化学療法の安全性および有用性を検証し、本邦における術後化学療法レジメンの妥当性を検討する。

3)臨床病期(c-Stage)IB-II 非小細胞肺癌(NSCLC)に対する術前化学療法の有用性を検討する。

1.　本研究の必要性:

当該疾患の標準的治療は外科的切除もしくは外科切除＋術後補助療法であるが、治療成績は不満足であり、より安全な全身治療の強化による治療成績の向上が期待される。最近、プラチナを用いた術後化学療法の有用性が当該病期において明らかになり、世界的に術後補助化学療法が「標準的治療」の一角を担いつつある。本邦では当該病期の一部(IB)の術後補助療法としてテガフール・ウラシル(UFT)の有効性が明らかになったが、欧米では当該病期に対してプラチナ製剤を含む 2 剤併用療法を標準的レジメンとしている。後者は本邦における安全性は確立しておらず、まずは標準的治療群に組み込まれるべき治療レジメンを決定する大規模比較試験が必要である。一方、術後化学療法の治療完遂率は50～85%であり、術前では90%以上のそ

れが期待できる。プラチナを用いた化学療法の有効性、安全性を考えれば、依然術前化学療法は有望であり、その治療意義を検証する必要がある。

2. 本研究の特色:

1) 欧米では進行病期に汎用される化学療法を用いて同様の症例を対象に術前化学療法と切除単独の比較試験を開始しているが、その化学療法の妥当性については検討されていない。
2) UFT に関する臨床試験は海外になく、欧米では同様の試験デザインで臨床試験が進む予定はない。

B. 研究方法

前研究では、臨床病期 IB-II 非小細胞肺癌症例に対して Cisplatin+Docetaxel (DC)と Docetaxel (D)単剤という二種類の化学療法のいずれかを行い、一年無再発生存割合、治療完遂率、治癒切除率、治療関連合併症をエンドポイントとして大規模試験に適当な術前化学療法を選択する。登録症例数は 80 例。今年度、集積後 1 年の評価を行い、当該病期の術前化学療法における至適治療レジメンを決定する。次いで、本研究では、まず術後の標準的化学療法レジメンを決定する比較試験(研究A)を行った後、先に決定された術前化学療法＋手術群を手術＋術後補助療法群を対照とした比較試験(研究B)で検証する。エンドポイントは生存率もしくは無再発生存割合。研究Aの予定登録は 1 群 300 例、合計 600 例; 2 年間で症例集積を行い、集積終了時点で中間解析を行う。引き続き、研究 B を行う。ここでもエンドポイントは生存率。予定登録は 1 群 150 例、合計 300 例; 2 年間で症例集積を行い、集積終了時点で中間解析を行う。5 年生存率を算定できるまで症例集積治療及び追跡を行って最終解析を行う。

(年度別研究計画):

第1年度:前研究の結果解析。次期臨床研究 A のプロトコール作成

第2年度:研究 A の試験実施計画書の作成

第3年度(当該年度):研究 A の試験実施計画書の作成、症例集積、治療。

3年計画終了時に研究継続が認められた場合、5年生存率を算定できるまで症例集積治療及び追跡を行って最終解析を行う。

(倫理面への配慮)

参加患者の安全性確保については、毒性中止・無効中止基準等の配慮がなされており、試験参加による不利益は最小化される。

また、ヘルシンキ宣言や米国ベルモントレポート等の国際的倫理原則に従い、これを遵守する。研究の監視:本研究班により、もしくは賛同の得られた他の主任研究者と協力して、臨床試験審査委員会、効果・安全性評価委員会、監査委員会を組織し、研究開始前および研究実施中の第三者的監視を行う。

臨床試験登録の際しては、この治療法が臨床試験であること、標準治療は手術単独であること、また術前治療を行うことに伴うメリット・リスク・不利益などを十分に説明がなされ、患者本人からの文書による同意を必須とする。また、試験の開始にあたり、グループ臨床試験審査委員会、参加各施設倫理委員会(IRB)の承認を得る。

C. 研究結果

本年度の研究では、標準的治療群に組み込まれるべき術後補助化学療法のレジメンを決定する臨床第Ⅲ相試験のデザインと実施計画書の作成を行った。本臨床第Ⅲ相試験の対象は、標準的外科切除を行った後に、病理病期ⅠB-ⅢA 期非小細胞肺癌と診断された症例とする。本試験は、術後 4 週から 8 週までの間に症例登録を行って、UFT 250mg/m2 の内服治療を開始し、2 年間継続する治療法(標準的治療群)、もしくは欧米で評価されたプラチナ化合物を含む 2 剤併用化学療法の一つであるカルボプラチンとパクリタキセル(CP 療法)を 4 コース行う治療法(試験治療群)のどちらかに無作為に割り付けて、それらの有効性を比較、検証する。エンドポイントは3年生存率もしくは無再発生存割合とし、予定登録は 1 群400 例、合計800 例、2 年間で症例集積を行い、集積終了時点で中間解析を行うデザインとした。一方、CP 療法について、術後補助療法としての投与量も含め安全性情報が不足していることから、グループ関連の施設で個別に臨床第Ⅱ相試験を実施した。試験は、進行肺癌で用いられる full dose の CP 療法が術後補助療法として可能か否かというデザインと卵巣癌等で用いられている投与量(full dose から約 10%、投与量を削減したもの)における安全性の検証を行うデザインの 2 種に分かれて実施した。いずれも primary endpoint は治療完遂率である。前者(WJTOG3105)は、完全切除された IB 期～IIIA 期非小細胞肺癌を対象に、step1 の試験用量・用法をカルボプラチン:

AUC=6、パクリタキセル 200mg/m2 を 3 週間毎に 1 回投与と規定した。集積症例数は 20 例、7 例登録時点で認容性の中間解析を行い、7 例中 5 例の認容性が確認された場合にはそのままの投与量で試験を継続し、認容性が確認されなければパクリタキセルを 175mg/m2 に減量(step2)して認容性を再評価するデザインで行った。本試験では「治療完遂率が 70%以上、G3 以上の末梢神経障害の発現が 30%以下」であれば「認容性あり」と判断すると規定した。本試験の結果は、①治療完遂例は 13/20 例(65%)、②減量をともなわない完遂例は 10 例(50%)、③18 例(90%)で 3cycle 以上施行可能、④中止例 6 例のうち 3 例が骨髄抑制に起因。⑤5 例で投与スケジュールの変更が必要、⑥Grade 3 の末梢神経障害の発現は 1 例(5%)であり、当初規定した full-dose の CP 療法の認容性は証明されなかった。他方、肺葉切除以上の手術が施行された IB～III 期非小細胞肺癌を対象にカルボプラチン:AUC=5、パクリタキセル 175mg/m2 を 4 サイクル施行する認容性試験を行った(LOGIK0501)。閾値完遂率:50%、期待完遂率:80%、$\alpha=0.05$、$\beta=0.1$ と仮定し、目標症例数を 30 例とした。本試験の結果は①完遂率は 79.4%、②脱落例は 20.6%で、高い認容性が示された。また、本試験のサブ解析から、65 歳以上の高年齢層でも同等の認容性が証明された。以上の結果から、次期多施設共同臨床試験で CP 療法を採用するなら、その投与量は full-dose よりも 15%程度減量したものを採択すべきであることが示唆された。これらの情報から第Ⅲ相試験ではより完遂率が高く安全と思われる投与量を決定する。

D. 考察

本邦からⅠ期非小細胞肺癌(腺癌)に対する UFT の術後化学療法の大規模臨床試験(N Eng J Med 2004; 350: 1713)と meta-analysis(J Clin Oncol 2005; 23: 4999)の結果が公表され、本邦においては UFT を用いた術後補助療法が少なくともⅠB 期の標準的治療戦略となりうる可能性が高いことが示された。また本剤が大腸癌や胃癌などの他癌種でも同様に補助療法として有効性が示された。従来進行肺癌での単剤としての有効性は 6～8%と言われていた薬剤が術後補助療法として有効性が示されたことは画期的である。当初、本研究では、これを標準治療として、進行肺癌で汎用され有効性が示されている CP 療法の有効性を検討するデザインとした。しかしながら、2006 年 6 月の米国臨床腫瘍学会(ASCO)において、シスプラチンを含む 2 剤併用療法による術後化学療法のメタアナリシス:Lung Adjuvant Cisplatin Evaluation(LACE)の結果と対象を臨床病期 IB 期に特化した CALGB9633 の追加報告がなされ、病期によっては化学療法のリスクがベネフィットを上回る可能性が示唆され、術後化学療法によって IA 期ではむしろ死亡リスクが高くなり、ⅠB 期では生存の延長に寄与することに疑問を残す結果であった。以上の経緯を踏まえグループ内で議論した結果、対象集団をプラチナ製剤の有効性が示された II、III 期と本邦においてのみ有効性が示された IB 期に分けて、新たに大規模臨床試験を計画する方針とした。IB 期においては UFT 投与群を対照として経口抗がん剤であるテガフール・ギメラシル・オテラシルカリウム配合剤(S-1)の有用性を評価する試験を、II-IIIA 期に対しては、プラチナ製剤を含む 2 剤併用療法投与群を対照として経口剤もしくは分子標的薬剤の維持療法としての上乗せ効果を検証する試験をそれぞれ検討中である。

これは術後補助療法として比較的毒性の少ない抗がん剤を長期投与することが良いのか、あるいは相応の毒性のある抗がん剤を進行癌と同様に短期的に投与するのが良いのかという術後補助治療コンセプトあるいは効果のメカニズムに関わる重要な情報を提供する可能性があり、研究の意義は大きい。また、この試験の結果は手術対象病期の非小細胞肺癌の標準的治療を確立するものであり、一般診療に情報還元するとともに、今後の臨床試験のデザインの礎となると予想される。

E. 結論

本研究(研究 A)は、2007年 3 月末現在試験実施計画書作成中であり、本研究の結論は得られなかった。

F. 健康危険情報

健康危険情報として該当する事項はない。

G. 研究発表

1. 論文発表

1) Saji, H., Song, W.*, Furumoto, K.*, Kato, H., Engleman, E. G.*Systemic antitumor effect of intratumoral injection of dendritic cells in combination with local photodynamic therapy., Clin Cancer Res 12:2568-2574 2006

2) Nitadori, J., Ishii, G., Tsuta, K., Yokose, T., Murata, Y., Kodama, T., Nagai, K., Kato, H., Ochiai, A., Immunohistochemical Differential Diagnosis Between Large Cell Neuroendocrine Carcinoma and Small Cell Carcinoma by Tissue Microarray Analysis With a Large Antibody Panel, Ameican Journal of Clinical Pathology 125(5):682-92 2006

3) Saijo, T., Ishii, G., Nagai, K., Funai, K., Nitadori, J., Tsuta, K., Nara, M., Hishida, T., Ochiai, A., Differences in clinicopathological and biological features between central-type and peripheral-type squamous cell carcinoma of the lung, Lung Cancer 52(1):37—45 2006

4) Hirano ,T., Kato ,H. Present status of clinical proteomic analysis for the early detection and determination of therapeutic strategy in lung cancer, Ann Thorac Cardiovasc Surg 12: 4-9, 2006

5) Rusch, VW., Tsuchiya, R., Tsuboi, M., Pass, HI., Grunenwald, D., Goldstraw, P., Surgery for bronchioloalveolar carcinoma and "very early" adenocarcinoma: an evolving standard of care?, J Thorac Oncol. 1: S27-S31, 2006

6) Ohira, T., Suga, Y., Nagatsuka, Y., Usuda, J., Tsuboi, M., Hirano, T., Ikeda, N., Kato, H. Early-stage lung cancer: diagnosis and treatment. Int J Clin Oncol. Feb;11(1):9-12. 2006

7) Tsuboi, M., Kato, H., Ichinose, Y., Ohta, M., Hata, E., Tsubota, N., Wada, H., Hamada, C., Hamajima, N., Ohta, M., On behalf of the Japan Lung Cancer Research Group (JLCRG) on Postsurgical Adjuvant Chemotherapy, The influence of tumor size, histological differentiation and smoking history in patients with completely resected stage I adenocarcinoma of the lung; Subset analyses of the Japan Lung Cancer Research Group (JLCRG) trial, J Clin Oncol. 24: 413S, 2006

8) 加藤 治文, (監訳:加藤 治文, 池田 徳彦, 坪井 正博, 編:Fossella, F.V., Komaki, R., Putnam, J.B. Jr.) MD アンダーソン癌センターに学ぶ癌治療 肺癌, シュプリンガ・ジャパン株式会社, 2006

2. 学会発表

1) Kato, H., The role of molecular markers, The 15th International conference on Screening for Lung Cancer (2006.10.20) New York, USA

2) Tsuboi, M., Kato, H., Adjuvant chemotherapy for stage I NSCLC in Japan, IASLC Workshop on Stereotactic Radiation Therapy and Surgery for Stage I Non-Small Cell Lung Cancer (2006.2.18) Hawaii, USA

3) Tsuboi, M., Asamura, H., Kato, H., Japanese clinical trials; ongoing & closed studies, 19th annual meeting of General Thoracic Surgical Club (2006.3.9) Arizona, USA

4) Tsuboi, M., Kato, H., Adjuvant chemotherapy in early stage NSCLC, 2nd international lung cancer symposium (2006.7.8) Nara

5) Tsuboi, M., Kato, H., A case for change: Data from the Japanese Joint Committee of Lung Cancer Registry of 6,644 resected cancers, CHEST 2006 (2006. 10.26) Salt Lake City, USA

6) Tsuboi, M., Kato, H., Japanese experiences with EGFR-TKIs, 3rd IASLC/ASCO/ESMO International Conference onTargeted Therapies in Lung Cancer (2006.11.9) Sicily, Italy

7) Tsuboi, M., Kato, H., The adjuvant chemotherapy in early stage non-small cell lung cancer; Taxol adjuvant therapy in 2006, KASLC autumn meeting 2006 (2006.11. 18) Seoul, Korea

8) Tsuboi, M., Kato, H., Ichinose, Y., Ohta, M., Hata, E., Tsubota, N., Wada, H., Hamada, C., Hamajima, N., Ohta, M., On behalf of the Japan Lung Cancer Research Group (JLCRG) on Postsurgical Adjuvant Chemotherapy, The influence of tumor size, histological differentiation and smoking history in patients with completely resected stage I adenocarcinoma of the lung; Subset analyses of the Japan Lung Cancer Research Group (JLCRG) trial, 42nd Annaul meeting, American Society of Clinical Oncology (ASCO) (2006.6.2-6) Atlanta, USA

9) Ohira, T., Usuda, J., Suga, Y., Miyajima, K., Nakajima, N., Oikawa, T., Kataba, H., Kojika, M., Saji, H., Tsuboi, M., Hirano, T., Kato, H., Molecular characterizations in clinical non-small-cell lung cancer (NSCLC) samples

obtained during surgery, 97th American Association for Cancer Research (2006.4.4) Washington DC

10) Miyajima, K., Ohira, T., Usuda, J., Saji, H., Tsuboi, M., Hirano, T., Kato, H., Suzuki, M., Toyooka, S., A .F. Gazdar*, The relationship between RASSF1A aberrant methylation and survival in small sized lung adenocarcinoma, 42nd American Society of Clinical Oncology (2006.6.2-6) Atlanta, Georgia,U.S.A.

11) Miyajima, K., Ohira, T., Suga, Y., Takahashi, M., Usuda, J., Nagatsuka, Y., Kajiwara, N., Uchida, O., Tsuboi, M., Hirano, T., Kato, H., A. F Gazdar*, The Relationship Between RASSF1A Aberrant Methylation And Survival In Small Sized Lung Adenocarcinoma., 86th American Association for Thoracic Surgery (20064.29-5.3) Philadelphia,PA, U.S.A.

12) Tsuboi, M., Kato, H., JCOG LCSSG ongoing & planning trials, Korean Lung Cancer Surgical Study meeting (2006.8.24) Seoul, Korea

13) 加藤 治文, 肺癌の診断と治療, 第47回日本臨床細胞学会総会学術集会 (2006.6.9) 横浜

14) 加藤 治文, 肺癌治療の現状と外科治療, 第 7 回肺がん撲滅デー市民公開講座「専門医が勧める肺がん治療」(2006.11.25) 東京

15) 加藤 治文, 局所限局非小細胞肺がんの集学的治療に関する研究, がん臨床研究・研究成果発表会(厚生労働省科学研究費研究成果等普及啓発事業) (2006.1.16) 東京

H. 知的財産権の出願・登録状況(予定を含む。)

1. 特許取得:特記すべき事項なし。
2. 実用新案登録:特記すべき事項なし。
3. その他:特記すべき事項なし。

別紙5

研究成果の刊行に関する一覧表

雑誌

発表者氏名	論文タイトル名	発表誌名	巻号	ページ	出版年
Saji, H. Song, W.*, Furumoto, K.*, Kato, H., Engleman, E. G.*	Systemic antitumor effect of intratumoral injection of dendritic cells in combination with local photodynamic therapy.	Clin Cancer Res	12	2568-2574	2006
Nitadori, J. Ishii, G., Tsuta, K., Yokose, T., Murata, Y., Kodama, T., Nagai, K., Kato, H., Ochiai, A.	Immunohistochemical Differential Diagnosis Between Large Cell Neuroendocrine Carcinoma and Small Cell Carcinoma by Tissue Microarray Analysis With a Large Antibody Panel	Ameican Journal of Clinical Pathology	125(5)	682-692	2006
Saijo, T. Ishii, G., Nagai, K., Funai, K., Nitadori, J., Tsuta, K., Nara, M., Hishida, T., Ochiai, A.	Differences in clinicopathological and biological features between central-type and peripheral-type squamous cell carcinoma of the lung	Lung Cancer	52(1)	37-45	2006
Hirano ,T. Kato ,H.	Present status of clinical proteomic analysis for the early detection and determination of therapeutic strategy in lung cancer	AnnThorac Cardiovasc Surg	12	4-9	2006
Rusch, VW. Tsuchiya, R., Tsuboi, M., Pass, HI., Grunenwald, D., Goldstraw, P.	Surgery for bronchioloalveolar carcinoma and "very early" adenocarcinoma: an evolving standard of care?	J Thorac Oncol	1	S27-S31	2006
Ohira, T. Suga, Y., Nagatsuka, Y., Usuda, J., Tsuboi, M., Hirano, T., Ikeda, N., Kato, H.	Early-stage lung cancer: diagnosis and treatment.	Int J Clin Oncol	Feb;11(1)	9-12.	2006
Tsuboi, M. Kato, H., Ichinose, Y., Ohta, M., Hata, E., Tsubota, N., Wada, H., Hamada, C., Hamajima, N., Ohta, M., On behalf of the Japan Lung Cancer Research Group (JLCRG) on Postsurgical Adjuvant Chemotherapy	The influence of tumor size, histological differentiation and smoking history in patients with completely resected stage I adenocarcinoma of the lung; Subset analyses of the Japan Lung Cancer Research Group (JLCRG) trial	J Clin Oncol	24	413S	2006

Systemic Antitumor Effect of Intratumoral Injection of Dendritic Cells in Combination with Local Photodynamic Therapy

Hisashi Saji,[1,3] Wenru Song,[2] Katsuyoshi Furumoto,[1] Harubumi Kato,[3] and Edgar G. Engleman[1]

Abstract

Purpose: Photodynamic therapy (PDT), which is used clinically for the palliative treatment of cancer, induces local tumor cell death but has no effect on tumors in untreated sites. The purpose of this study was to determine if local PDT followed by intratumoral injection of naïve dendritic cells (IT-DC) induces systemic antitumor immunity that can inhibit the growth of untreated as well as PDT + IT-DC – treated tumors.

Experimental Design: BALB/c or C57Bl/6 mice were injected s.c. with CT26 colorectal carcinoma cells and B16 melanoma cells, respectively, and following 10 to 12 days of tumor growth, the tumors were treated with PDT alone or PDT followed by IT-DC or IT-PBS. In other studies, tumors were established simultaneously in both lower flanks or in one flank and in the lungs, but only one flank was treated.

Results: Whereas neither PDT nor IT-DC alone was effective, PDT + IT-DC eradicated both CT26 and B16 tumors in a significant proportion of animals and prolonged the survival of mice of which the tumors were not cured. The spleens of mice treated with PDT + IT-DC contained tumor-specific cytotoxic and IFN-γ-secreting T cells whereas the spleens of control groups did not. Moreover, adoptive transfer of splenocytes from successfully treated CT26 tumor-free mice protected naïve animals from a subsequent challenge with CT26, and this was mediated mainly by CD8 T cells. Most importantly, PDT plus IT-DC administered to one tumor site led to tumor regression at distant sites, including multiple lung metastases.

Conclusions: PDT + IT-DC induces potent systemic antitumor immunity in mice and should be evaluated in the treatment of human cancer.

Dendritic cells (DC) are the most potent antigen-presenting cells known, uniquely capable of activating both the cognate and innate arms of the immune system. For example, administration of DCs loaded *ex vivo* with tumor-associated antigens can elicit antitumor immunity resulting in tumor regression in various murine models, and DCs pulsed with tumor derived peptides, proteins, genes or lysates, as well as DCs fused with tumor cells, have all been studied as therapeutic cancer vaccines (1–11). Although the methods are complex and costly to implement, promising results have been obtained in clinical trials in patients with advanced malignancies. These trials have shown DC-based vaccination to be well tolerated and capable of inducing tumor-specific T-cell responses and regression of metastatic disease. On the other hand, the overall therapeutic efficacy of this approach has been limited, indicating a need to either enhance its potency or combine it with other treatment modalities.

Among the modalities that might be combined with DC-based immunotherapy are systemically administered antitumor drugs as well as locally targeted therapies such as radiation, radiofrequency ablation, and photodynamic therapy (PDT). PDT has been approved in the United States and other countries as an anticancer therapy, mainly for the palliative treatment of surgically inaccessible tumors. PDT involves the systemic administration of a photosensitizer that preferentially accumulates in transformed cells, followed by illumination of the tumor with a laser beam (12). In the presence of oxygen, the laser light activates the photosensitizer and initiates a complex photochemical reaction that generates cytotoxic intermediates. Tumor destruction after PDT results from direct cytotoxic effects as well as from the induction of a local inflammatory response (12). Thus, preclinical studies have shown that PDT not only mediates apoptotic and necrotic killing of tumor cells but also alters the tumor microenvironment through the release of proinflammatory cytokines such as tumor necrosis factor α, interleukin (IL)-1 and IL-6 (12, 13).

On the basis of its unique mechanism of tumor destruction, PDT has the potential to create an environment at the tumor site that favors both tumor antigen loading and activation of DCs, key requirements for induction of antitumor immunity (14). Because most tumors lack an abundance of DCs, one way to potentially take advantage of this environment would be to inject a sufficient number of autologous DCs directly into

Authors' Affiliations: Departments of [1]Pathology and [2]Medicine, Stanford University School of Medicine, Palo Alto, California and [3]Department of Surgery, Tokyo Medical University, Tokyo, Japan

Received 9/12/05; revised 1/5/06; accepted 1/19/06.

Grant support: National Heart, Lung, and Blood Institute grant HL57443 (E.G. Engleman) and NIH National Cancer Institute grant K08CA105064 (W. Song).

The costs of publication of this article were defrayed in part by the payment of page charges. This article must therefore be hereby marked *advertisement* in accordance with 18 U.S.C. Section 1734 solely to indicate this fact.

Note: H. Saji and W. Song contributed equally to this work.

Requests for reprints: Edgar G. Engleman, Stanford Blood Center, 3373 Hillview Avenue, Palo Alto, CA 94304-1204. Phone: 650-723-7960; Fax: 650-725-0592; E-mail: edengleman@stanford.edu.

doi:10.1158/1078-0432.CCR-05-1986

PDT-treated tumors. Such a strategy alleviates the need to do *in vitro* loading of DCs with tumor antigens because the inflammatory milieu induces DC activation, which facilitates not only antigen acquisition and processing but also migration of the DCs to draining lymph nodes where they interact with a broad range of potential effector cells. In the current study, we evaluated the effect of combining PDT with intratumoral injection of syngeneic DCs (IT-DC) on two histologically distinct murine tumors, CT26 colon carcinoma and B16 melanoma. The results show that this combined treatment induces strong and durable tumor-specific immunity that results in the destruction not only of targeted tumors but also of tumors at distant sites.

Materials and Methods

Mice. Female BALB/c (H-2^d) and C57Bl/6 (H-2^b) mice, 6 to 8 weeks of age, were purchased from The Jackson Laboratory (Bar Harbor, ME). All mice were housed in the Stanford animal facility in accordance with the NIH guidelines.

Cell lines. The murine CT26 colon carcinoma, B16 melanoma (F10 clone), MAD109 lung carcinoma, and EL-4 lymphoma cell lines used in this study were maintained in complete RPMI 1640 with 10% fetal bovine serum, penicillin G (100 units/mL), streptomycin (100 μg/mL), and L-glutamine (10 mmol/L).

DCs. Bone marrow–derived DCs were generated in the presence of granulocyte macrophage colony-stimulating factor and IL-4 for 7 days as previously described (15). Bone marrow cells were harvested from femurs and tibias, and after RBC lysis, the resulting cell suspension was incubated in complete RPMI 1640 containing recombinant murine granulocyte macrophage colony-stimulating factor (10 ng/mL; PeproTech, Inc., Rocky Hill, NJ) and recombinant murine IL-4 (10 ng/mL; PeproTech). On day 2, nonadherent granulocytes were gently removed and fresh medium with granulocyte macrophage colony-stimulating factor and IL-4 was added. On day 5, loosely adherent cells were dislodged and replated. On day 7 of culture, the unpulsed DCs were collected. The maturational status and percentage of DCs were verified by flow cytometry, and staining of three surface markers (CD11c, CD86, and class II antigen) showed the purity of DCs to be ≥74%.

Photosensitizer and laser unit. ATX-S10 Na(II), a hydrophilic chlorin photosensitizer with an absorption maximum at 670 nm (16), was obtained from Photochemical Co. Ltd. (Okayama, Japan). A diode laser (Hamamatsu Photonics, Hamamatsu, Japan) was used as a light source for exciting ATX-S10 Na(II). The diode laser is a continuous-wave laser operating at 670-nm wavelength.

During the light irradiation, mice were anesthetized with ketamine (125 mg/kg: Vedco, Inc., St. Joseph, MO) and xylazine (25 mg/kg; Phoenix Pharmaceutical, Inc., St. Joseph, MO) and were restrained in a specially designed holder.

Combined PDT and IT-DC therapy of CT26 colon cancer. Preliminary studies with ATX-S10 Na(II) and a diode laser, were carried out on the basis of a published protocol (16) to identify a drug dose and laser setting for inhibition of growth of CT26 tumors *in vivo* without major local or systemic toxicity. CT26 tumor cells (10^6 per mouse) in 100 μL HBSS were injected into the lower right flank of BALB/c mice. On day 12, when the average tumor volume was 153.0 ± 11.5 mm^3, the mice received an i.v. injection of ATX-S10 Na(II) (5 mg/kg body weight), followed 4 to 5 hours later by 150 J/cm^2 laser irradiation of the tumor. DCs (1×10^6 per injection in 50 μL PBS) were injected into the tumor on days 13, 14, 15, and 17. The tumor volume was measured thrice a week using a caliper [tumor volume (mm^3) = (longer diameter) × (shorter diameter)^2 × 0.4]. Animals were sacrificed when the tumor diameter exceeded 20 mm or when there were signs of animal distress. Survival was recorded as the percentage of surviving animals on a given day. Surviving mice had no sign of tumor when experiments were terminated.

Combined PDT and IT-DC therapy of B16 melanoma. For the B16 melanoma tumor model, C57Bl/6 mice were inoculated s.c. with 5×10^5 tumor cells in the lower right flank. On day 10, mice with established tumors (average tumor volume, 80.0 ± 5.4 mm^3) were treated with 150 J/cm^2 laser irradiation to the tumor 4 to 5 hours after an ATX-S10 Na(II) (5 mg/kg body weight) injection and given intratumoral injections of DCs on days 11, 12, 13, and 15 (1×10^6 per injection in 50 μL PBS). The measurement of tumor volume and survival was as above.

ELISPOT assays. ELISPOT assays were done with an ELISpot mouse IFN-γ system (R&D Systems, Inc., Minneapolis, MN) according to the instructions of the manufacturer. Splenocytes were isolated 4 weeks after tumor inoculation. After lysis of RBC, splenocytes were resuspended at a final concentration of 5×10^5/mL and 100 μL of this suspension were then incubated at 37°C for 24 hours in ELISPOT plates coated with anti-IFN-γ with 100 μL medium with or without irradiated (30 Gy) stimulator cells (CT26, MAD109, B16, or EL-4).

Cytotoxicity assays. Cytotoxicity was measured by a standard chromium-51(^{51}Cr) release assay. Splenocytes were harvested 4 weeks after tumor inoculation. After lysis of RBC, splenocytes (1×10^6/mL) were stimulated *in vitro* by irradiated (100 Gy) tumor cells (1×10^5/mL) at 37°C for 5 days in the presence of 10 units/mL IL-2. Following culture, splenocytes were separated from dead cells and debris with Lympholyte-M cell separation media (Cederlane Laboratories, Inc., Hornby, Ontario, Canada). Target cells were labeled with ^{51}Cr (200 μCi/5×10^6 cells) for 1 hour at 37°C, washed, and then incubated in U-bottomed wells with effector cells at various effector-to-target cell ratios at 37°C for 4 hours. Spontaneous release and maximum release were determined by incubating target cells in medium alone or in 1% SDS, respectively. Spontaneous release was always <20% of maximum. Radioactivity was counted in a liquid scintillation counter and the percentage of specific target cell lysis was calculated with the formula $[(E - S) / (T - S)] \times 100$, where E is the average experimental release, S is the average spontaneous release, and T is the average maximal release.

Adoptive transfer of splenocytes. To determine whether lymphocytes induced by PDT + IT-DC could protect naïve animals from a tumor challenge, BALB/c mice were inoculated s.c. with CT26 cells and treated with PDT + IT-DC as before. Four weeks later, the splenocytes were harvested and 1×10^7 cells were infused i.v. into naïve mice. Control groups of mice received splenocytes from CT26 tumor-bearing mice treated with either IT-PBS alone, IT-DC alone, or PDT + IT-PBS. One day later, these mice were s.c. challenged with a lethal number (1×10^6) of CT26 cells and monitored for tumor volume and survival.

To analyze the role of specific T-cell subsets in tumor protection, splenocytes were harvested from inoculated tumor-free mice treated with PDT + IT-DC, and $CD4^+$ or $CD8^+$ T cells were depleted by using CD4 (L3T4) or CD8a (Ly-2) coupled microbeads and magnetic cell sorting (Miltenyi Biotec, Inc., Auburn, CA). Splenocytes, $CD4^+$ T-cell–depleted splenocytes, or $CD8^+$ T-cell–depleted splenocytes (1×10^7) were infused i.v. into groups of five naïve mice. Control mice received splenocytes from naïve mice. One day later, the mice were s.c. challenged with a lethal number (1×10^6) of CT26 cells and monitored for tumor volume and survival. These depletion conditions were validated by flow cytometry analysis using anti-CD4 (L3T4)-FITC and CD8a (Ly-2)-phycoerythrin monoclonal antibodies (PharMingen, San Diego, CA). The percent depletion of $CD4^+$ and $CD8^+$ cells was 97% and 93%, respectively.

Secondary tumor challenge. To determine the persistence of tumor-specific immunity in the mice treated by PDT + IT-DC, at day 60 after first tumor inoculation, mice showing complete regression of CT26 tumors were given a second s.c. tumor challenge (1×10^6 CT26) in the left lower flank (contralateral to the first injection site). These mice, as well as a control group of naïve mice that were inoculated with 1×10^6 CT26 tumor cells, were monitored for tumor size and survival.

Effect of PDT + IT-DC on contralateral tumors. To determine whether PDT + IT-DC treatment of one s.c. tumor affected an

established contralateral s.c. tumor, CT26 cells (1×10^6) were injected s.c. into both lower flanks of BALB/c mice on day 0. On day 12, tumor-bearing mice were either untreated or treated with combined PDT + IT-DC (using the protocol above) into the tumor on the right side but not into the tumor on the left side. The bilateral tumor-bearing mice were followed for tumor volume on both flanks.

Effect of PDT + IT-DC on multiple distant tumors. BALB/c mice were inoculated s.c. with 1×10^6 CT26 tumor cells on day 0. On day 5, these mice were injected i.v. with 1×10^6 CT26 tumor cells. PDT + IT-DC was administered on day 12 (as above) to the s.c. tumor alone. On day 21 after i.v. tumor inoculation, mice were euthanized and lungs were harvested and fixed with Bouin's solution (Sigma-Aldrich, St. Louis, MO).

Statistical analysis. Differences between groups were analyzed using unpaired two-tailed Student's *t* test. Survival curves were plotted by the Kaplan-Meier method and comparisons among groups in the survival data were calculated by log-rank test.

Results

Effect of combination treatment with PDT and IT-DC on CT26 tumors. To test the hypothesis that local PDT followed by IT-DC can inhibit primary tumor growth, BALB/c mice were injected s.c. with CT26 tumor cells. On day 12, the tumors reached an average diameter of 10.5 mm and could not be cured with PDT alone (data not shown). PDT was done at that time and syngeneic DCs were injected intratumorally 1 day later (day 13) and again on days 14, 15, and 17. Although the tumors grew rapidly following treatment with PBS alone, IT-DC alone, and PDT + IT-PBS, the combination of PDT + IT-DC resulted in significant suppression of tumor growth ($P < 0.05$ versus all other groups; Fig. 1A). Four of the nine (44%) animals treated with PDT + IT-DC became tumor-free and the overall survival of the PDT + IT-DC group was significantly prolonged compared with other groups (log-rank test, $P = 0.0006$; Fig. 1B). To determine if the combination of PDT + IT-DC results in immunologic memory, mice that had been treated with PDT + IT-DC and were tumor-free following an initial tumor inoculation were rechallenged in the opposite flank with a second lethal inoculation of the same tumor. The results show that these mice not only survived but were completely resistant to this second inoculation (Fig. 1C).

Effect of combination treatment with PDT and IT-DC on B16 tumors. In contrast to CT26 tumors, the B16 melanoma is considered poorly immunogenic and highly aggressive. Moreover, PDT for the treatment of melanoma has had only limited benefit (17), which is attributed to the presence in such tumors of a large amount of light-absorbing melanin pigment that prevents penetration of the laser beam into the tumor tissue. Our preliminary studies showed that PDT alone could not induce any suppression of growth of B16 tumors, even against s.c. tumors as small as 3 mm in diameter (data not shown). Surprisingly, PDT in combination with IT-DC resulted in a striking antitumor effect ($P < 0.05$, versus all other groups; Fig. 2A). Four of seven (57%) mice treated with PDT + IT-DC became tumor-free and the overall survival of the PDT + IT-DC group was significantly prolonged compared with other groups (log-rank test, $P = 0.0004$; Fig. 2B). Interestingly, two of four PDT + IT-DC–treated tumor-free mice developed white hair at sites of treatment, and in one of these mice, white hair could be seen at a site (neck) distant from the PDT site at ~40 days after treatment (Fig. 2C).

In vitro *characterization of the antitumor immune response induced by PDT + IT-DC.* A correlation between *in vitro* tumor-specific IFN-γ production by host-derived T cells and systemic antitumor immunity has been shown in other studies (18, 19). Using ELISPOT assays, we evaluated whether treatment of CT26 tumor-bearing mice with PDT + IT-DC could elicit tumor-specific IFN-γ-secreting T cells. As shown in Fig. 3A, splenocytes from mice treated with PDT + IT-DC contained significantly more tumor-specific IFN-γ-secreting cells than splenocytes from other groups ($P < 0.05$, versus other groups). Moreover, this cytokine was not secreted spontaneously or in response to

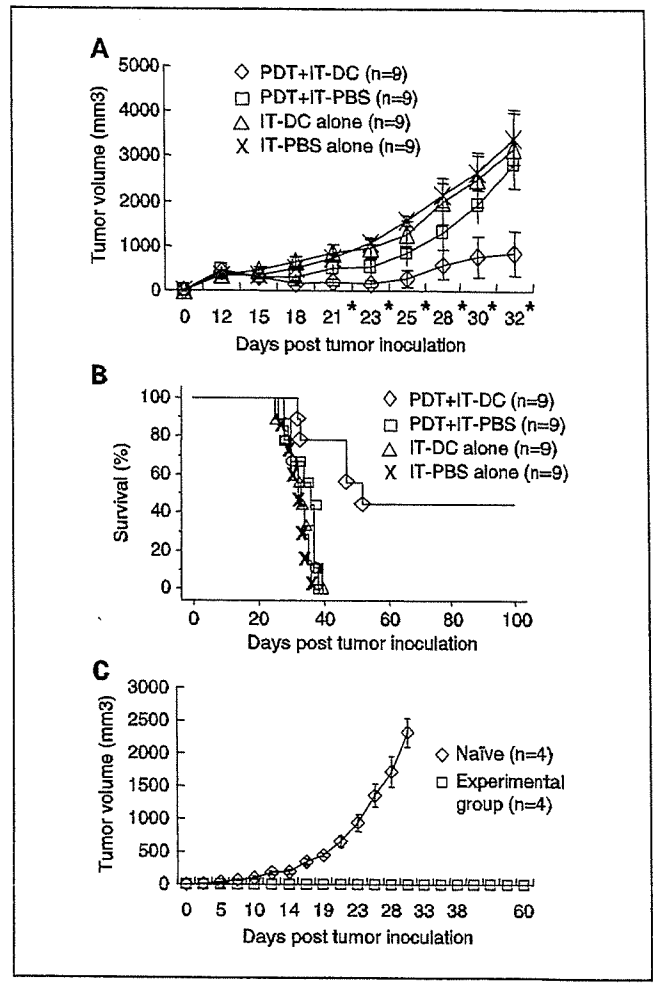

Fig. 1. Effect of combined PDT + IT-DC on the growth of established CT26 syngeneic colon carcinoma tumors. CT26 cells (1×10^6) were injected s.c. in the right lower flank of BALB/c mice. On day 12, mice with established tumors (mean tumor volume 153.0 ± 11.5 mm^3) were treated with PDT as described in Materials and Methods. DCs (1×10^6 in 50 μL PBS) were administered intratumorally on days 13, 14, 15, and 17. The experimental groups included intratumoral injection of PBS alone (50 μL, $n = 9$; ×); intratumoral injection of DCs alone ($n = 9$; △); PDT combined with intratumoral PBS ($n = 9$; □); and PDT combined with IT-DC ($n = 9$; ◇). *A*, mean tumor volume (mm^3) for treatment groups [mean tumor volume = (longer diameter) × (shorter diameter)^2 × 0.4]. Points, mean; bars, SE. *, $P < 0.05$, PDT + IT-DC versus other treatments. *B*, survival of mice recorded as the percentage of surviving animals on a given day. Surviving mice had no sign of tumor when the experiment was terminated. *C*, CT26 tumor rechallenge of tumor-free mice after PDT + IT-DC. Mice that had received CT26 inoculation followed by PDT + IT-DC were rechallenged s.c. with a lethal number (1×10^6) of CT26 tumor cells ($n = 4$; □). Naïve mice inoculated s.c. with the same number of CT26 cells served as controls ($n = 4$; ◇). Experiments were done thrice with similar results.

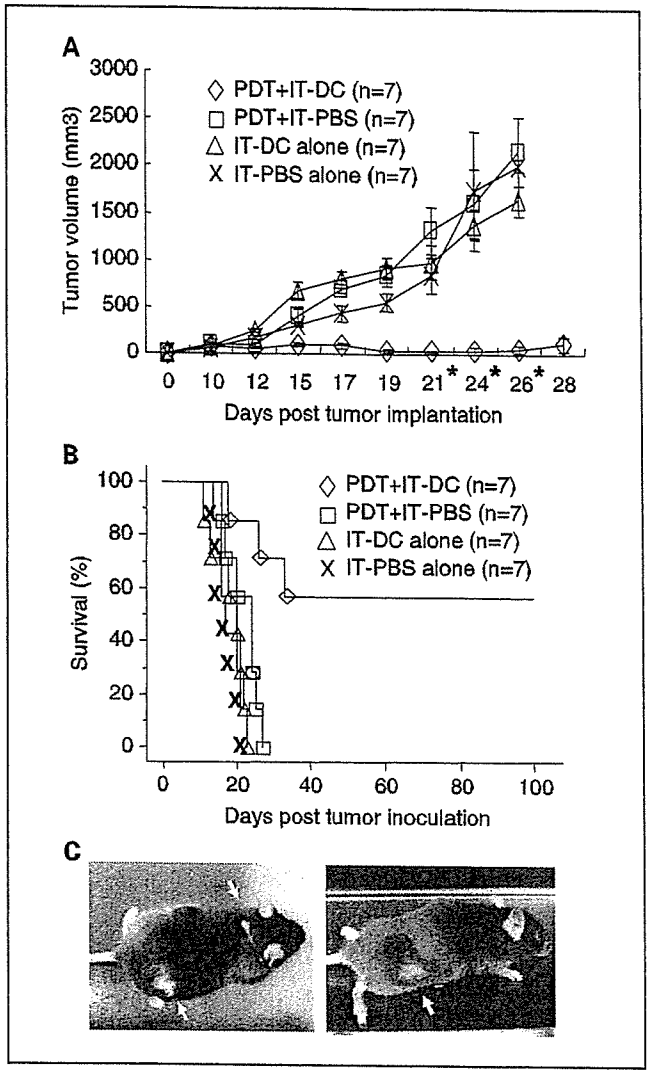

Fig. 2. Effect of PDT + IT-DC on the growth of established B16 melanoma tumors. B16 cells (5×10^5) were injected s.c. in the right lower flank of C57Bl/6 mice. On day 10, mice with established tumors (average tumor size, 80.0 ± 5.4 mm^3) were treated with PDTand received IT-DC (1×10^6 in 50 μL PBS) on days 11, 12, 13, and 15. The experimental groups included IT-PBS alone (50 μL, $n = 7$; ×); IT-DC alone ($n = 7$; △); PDT + IT-PBS ($n = 7$; □); and PDT + IT-DC ($n = 7$; ◇). *A*, mean tumor volume (mm^3) for treatment groups [mean tumor volume = (longer diameter) × (shorter diameter)^2 × 0.4]. Points, mean; bars, SE. *, $P < 0.05$, PDT + IT-DC versus other treatments. *B*, survival of mice recorded as the percentage of surviving animals on a given day. Surviving mice had no sign of tumor when the experiment was terminated. Experiments were done thrice with similar results. *C*, photographs of tumor-free mice taken 60 days after PDT + IT-DC treatment of B16 melanoma. Arrows, white hair growing in an untreated site (neck of mouse on left) and in treated sites (right flanks of both mice).

MAD109 cells, which are irrelevant syngeneic murine lung tumor cells, indicating that the observed response was immunologically specific to CT26 tumor cells. In additional studies, we analyzed the splenocytes of the different treatment groups for the presence of CT26-specific CTLs. Figure 3B shows that such cells were present in the PDT + IT-DC group but not in other groups ($P < 0.05$, versus all other groups). There was no killing of a syngeneic lung cancer cell line (MAD109), indicating that the CTLs are CT26 tumor specific (data not shown).

A tumor-specific immune response was also observed in B16 tumor–bearing mice that had been treated with PDT + IT-DC. As shown in Fig. 4A, splenocytes from such mice contained significantly more tumor-specific IFN-γ-secreting cells compared with splenocytes from control groups ($P < 0.05$). In addition, as shown in Fig. 4B, PDT + IT-DC induced tumor-specific CTLs, as indicated by the presence of such cells in treated but not control animals. No lysis of a syngeneic lymphoma cell line (EL-4) was observed, indicating those CTLs are B16 tumor specific (data not shown).

In vivo *characterization of the antitumor immune response induced by PDT + IT-DC.* To further evaluate the role of CTLs in PDT + IT-DC–induced tumor protection, splenocytes from CT26 inoculated PDT + IT-DC–treated tumor-free mice and splenocytes from control groups were transferred to naïve mice. One day later, the mice were inoculated with a lethal dose of

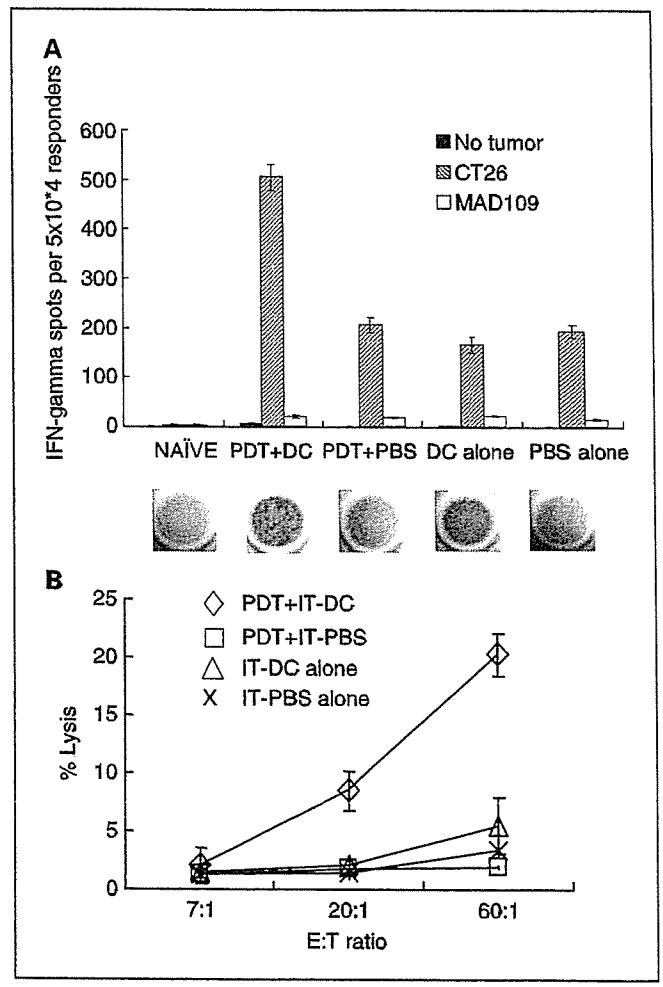

Fig. 3. Induction of *in vitro* anti-CT26 tumor immunity by PDT + IT-DC. *A*, CT26 tumor-bearing mice were treated as detailed in the legend to Fig. 1. Four weeks after tumor inoculation, splenocytes from treated, control, and naïve mice were incubated with or without specific tumor cells or MAD109, irrelevant irradiated tumor cells in an IFN-γ ELISPOTassay. Columns, average number of spots per 5×10^4 responders of triplicate samples; bars, SE. *, $P < 0.05$, versus other groups. Representative ELISPOTwells are shown below the graph. Data are from one of three representative experiments. *B*, CTLs in mice that had been inoculated with CT26 tumor cells followed by treatment with PDT + IT-DC. Four weeks after tumor inoculation, graded numbers of splenocytes from mice receiving various treatment protocols (×, IT-PBS alone; △, IT-DC alone; □, PDT + IT-PBS; ◇, PDT + IT-DC) were cultured in the presence of irradiated CT26 cells for 5 days. Cytotoxicity was measured with a standard 4-hour ^{51}Cr release assay at various ratios of effectors to targets using ^{51}Cr-labeled CT26 cells as targets.

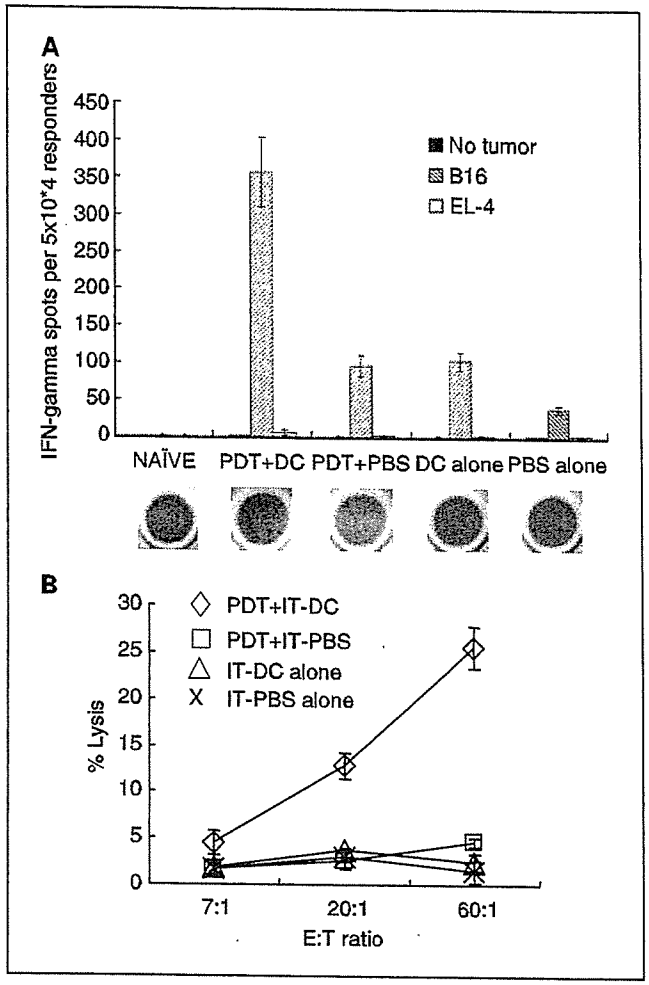

Fig. 4. Induction of anti-B16 tumor immunity by PDT + IT-DC treatment. *A*, B16 tumor–bearing mice were treated as detailed in the legend to Fig. 2. Four weeks after tumor inoculation, splenocytes from treated, control, and naïve mice were incubated with or without specific target cells or irrelevant irradiated tumor cells (EL-4) in an IFN-γ ELISPOT assay. Columns, average number of spots per 5×10^4 responders of triplicate samples; bars, SE. *, $P < 0.05$, versus other groups. Representative wells from an ELISPOT plate are shown below the graph. Data are from one of three representative experiments. *B*, CTLs in mice that received B16 tumor inoculation followed by treatment with PDT + IT-DC. Four weeks after tumor inoculation, graded numbers of splenocytes were cultured in the presence of irradiated B16 tumor cells for 5 days (×, IT-PBS alone; △, IT-DC alone; □, PDT + IT-PBS; ◇, PDT + IT-DC). Cytotoxicity was measured with a 4-hour ^{51}Cr release assay at various ratios of effectors to targets using ^{51}Cr-labeled B16 cells as targets.

CT26 tumor cells. Mice receiving splenocytes from the PDT + IT-DC–treated mice, but not from other mice, were protected from a subsequent tumor challenge with CT26 (Fig. 5A). To determine the role of $CD4^+$ and $CD8^+$ T cells in tumor protection, we repeated this experiment using whole splenocytes or splenocytes depleted of $CD4^+$ or $CD8^+$ T cells. Splenocytes from naïve mice were used as negative controls. One day later, these mice were s.c. challenged with a lethal number of CT26 tumor cells. As shown in Fig. 5B, whereas both $CD4^+$ and $CD8^+$ T cells from PDT + IT-DC–treated mice contributed to tumor protection, CD8 T cells mediated most of the effect.

Effect of PDT + IT-DC on distant untreated tumors. To determine whether treatment of one tumor with PDT + IT-DC conferred systemic antitumor effects, CT26 tumors were established simultaneously in both lower flanks, but only one site was treated with PDT + IT-DC. As shown in Fig. 6A, the growth of both tumors was significantly suppressed compared with the control group, showing that treatment of a primary tumor with PDT + IT-DC confers suppression of the growth of untreated as well as treated tumors. To simulate the clinical scenario in which multiple tumors are present at sites distant from the primary tumor, mice were simultaneously inoculated s.c. in one flank (as above) and i.v. with CT26 tumor cells. This resulted in the seeding of both lungs and the growth of multiple pulmonary metastases. Although a few lesions were visible in the lungs of mice treated with PDT + IT-DC, as shown in Fig. 6B, PDT + IT-DC treatment of the s.c. tumor in such mice resulted in a significant reduction of the lung lesions compared with untreated control animals ($P < 0.05$). Representative examples of lungs from a healthy mouse, a tumor-bearing PDT + IT-DC–treated mouse, and an untreated (control) tumor-bearing mouse are shown in Fig. 6C, D, and E.

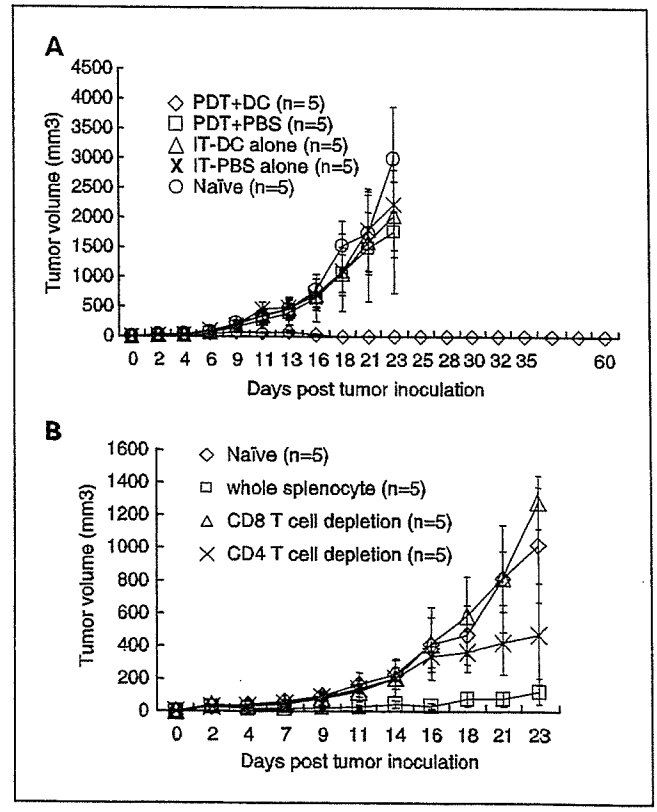

Fig. 5. *A*, adoptive transfer of splenocytes from PDT + IT-DC–treated mice to naïve mice prevents CT26 tumor growth. Splenocytes (1×10^7) from CT26 inoculated mice treated with IT-PBS alone (×), IT-DC alone (△), PDT + IT-PBS (□), or PDT + IT-DC (◇) were infused i.v. into naïve mice. One day later, the mice were challenged s.c. with a lethal number (1×10^6) of CT26 tumor cells. Naïve mice without splenocyte transfer were used as a control (○). Points, average tumor volume (mm^3) of five mice per group; bars, SE. *B*, role of CD4 and CD8 T-cell subsets in protection against CT26 tumors. Splenocytes were harvested from tumor-free mice treated with PDT + IT-DC. $CD4^+$ or $CD8^+$ T cells in splenocytes were depleted by using CD4 (L3T4) or CD8a (Ly-2) microbead magnetic cell sorting. After magnetic selection, whole splenocytes (□), CD4+ T-cell–depleted splenocytes (×), and CD8+ T-cell–depleted splenocytes (△) were infused i.v. into each of five naïve mice. Mice treated with splenocytes from naïve mice served as a control group (◇). One day later, these mice were s.c. challenged with a lethal number (1×10^6) of CT26 cells and monitored for tumor volume and survival.

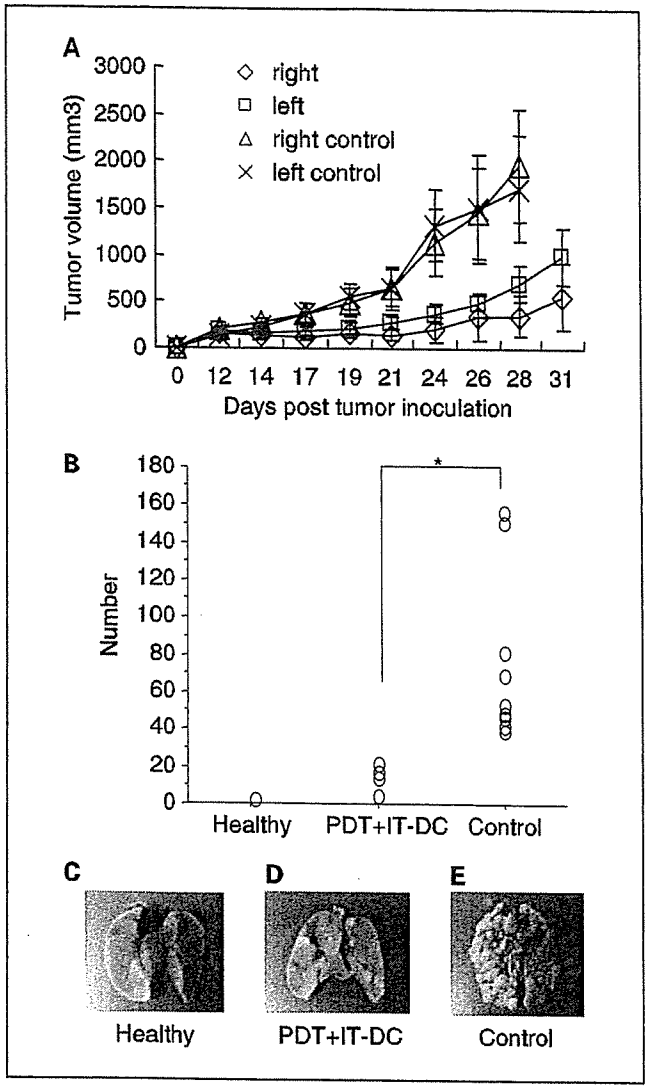

Fig. 6. Systemic tumor-specific immunity induced by local PDT + IT-DC treatment affects tumors at distant sites. *A*, CT26 tumor cells (1×10^6 for each side) were s.c. inoculated in both lower flanks of BALB/c mice. Twelve days later, the tumor-bearing mice were either untreated or treated with PDT + IT-DC into tumors on the right side but not the left side. Tumor growth on the left (untreated) and right (treated) sides was monitored and average tumor volume (±SE) was determined. Shown is the tumor volume on the right (with IT-PBS; △) and left (×) sides of control mice and the right (◇) and left (□) sides of treated mice. Each group contained five mice. *, $P < 0.05$, between left treated and control groups and between right treated and control groups. *B*, 10 BALB/c mice were inoculated s.c. with 1×10^6 CT26 tumor cells on day 0. On day 5, mice were injected i.v. with the same number of CT26 tumor cells, and on day 12, the s.c. tumors were treated with PDT + IT-DC. On day 26, lungs were harvested and stained with Bouin's solution to confirm and quantify lung metastases. *, $P < 0.05$, versus control group. *C*, representative lungs from a healthy mouse. *D*, representative lungs from a tumor-bearing PDT + IT-DC – treated mouse. *E*, representative lungs from an untreated control mouse.

Collectively, these data indicate that PDT + IT-DC therapy induces potent systemic tumor-specific immunity against CT26 colon cancer.

Discussion

One reason postulated for the limited clinical efficacy of most DC-based cancer vaccines studied to date is their variable ability to induce strong antitumor immunity, particularly CTL responses. This variability may have been due to problems related to tumor antigen selection or DC activation. Most DC-based clinical trials have included only a single or few tumor antigens although tumors contain thousands of potential antigens. Moreover, although a wide range of methods have been used to activate DCs and load them with antigens *in vitro*, there is no agreement about which of these methods induces optimal antitumor immunity. We sought to overcome these limitations by introducing unpulsed syngeneic DCs directly into tumors following treatment of the tumors with PDT, which creates a microenvironment that favors tumor antigen acquisition as well as activation of the DCs. The results confirm that PDT-treated tumors contain all of the factors necessary to activate DCs, load them with antigens, and induce an effective systemic antitumor immune response.

Although relatively little work has been done to evaluate the combination of PDT and IT-DC, several previous studies have shown the benefit of combining IT-DC with chemotherapy or radiotherapy (20–26). In contrast to chemotherapy or radiotherapy, PDT is not associated with systemic toxicity. Moreover, PDT renders murine tumors more immunogenic than tumors treated with UV or ionizing irradiation, or frozen and thawed tumors (27). Recently, Jalili et al. (28) reported that PDT in combination with IT-DC had little or no effect on s.c. CT26 tumors but inhibited the growth of contralateral tumors. By contrast, we observed dramatic effects on both local and distant tumors despite the fact that treatment was begun 12 days after inoculation of mice with a higher tumor dose than that studied by Jalili et al. One possible explanation for this surprising result is that we injected the same DC number four times as opposed to twice in their study. Another difference in our two studies is that Jalili et al. used the hematoprophyrin derivative, profimersodium (Photofrin), as a photosensitizer whereas we used ATX-S10 Na(II). Although Photofrin is widely used clinically, its potency is limited by weak absorbance at the shorter range of the red region of the spectrum. In addition, Photofrin is not a pure substance but a mixture of hematoporphyrin monomers, dimers, oligomers, and their dehydration products, and these products are associated with long-lasting skin photosensitivity (12). In contrast, ATX-S10 Na(II) is a homogeneous agent that preferentially accumulates in tumor tissues and is eliminated from normal tissues within 24 to 48 hours after injection. Moreover, its absorption maximum lies at 670 nm, which is longer than that of Photofrin (630 nm) and enables deeper tissue penetration (16). Using ATX-S10 Na(II) as a photosensitizer, we showed that PDT in combination with IT-DC inhibits the growth of two histologically distinct murine tumors. Interestingly, treatment of B16 tumors with combined PDT + IT-DC was at least as effective as it was for CT26, despite the poor immunogenicity of B16 and its well-documented resistance to PDT alone (29).

Our studies clearly show that PDT + IT-DC induces systemic antitumor immunity as well as tumor-specific immunologic memory. In the B16 model, the observation of white hair in untreated sites of mice, of which the tumors had been eradicated following PDT + IT-DC, suggests that treatment induced a systemic immune response against one or more shared antigens present in normal melanocytes as well as B16 tumors. In the CT26 model, PDT + IT-DC treatment of a single s.c. tumor resulted in regression of both contralateral as well as multiple

pulmonary tumors. The cells responsible for mediating tumor regression were cytotoxic T cells as indicated by both *in vitro* cytotoxicty assays and the observation that naïve animals were protected against tumors by adoptively transferred splenocytes from successfully treated tumor-bearing mice. Depletion of specific T-cell subsets (CD4 or CD8) in the adoptively transferred splenocytes indicated the CD8 T cells are the major effector cells induced by the PDT + IT-DC treatment.

Critical to the systemic antitumor effect of PDT + IT-DC is the capture of tumor-associated antigens by DCs as well as DC activation. Whether necrotic or apoptotic tumor cells serve as the superior source of tumor-associated antigens is controversial (30–34). Our data (not shown) strongly suggest that PDT, which induces both apoptosis and necrosis of tumors (12, 28), causes DCs to take up and process tumor antigen released by the dying tumor cells, mature, and become activated *in situ* and then cross-prime T cells against tumor-derived antigens. Interestingly, PDT alone had little or no effect on the growth of B16 tumors and analysis of such tumors following their treatment with PDT revealed a much smaller percentage of apoptotic and necrotic cells than in identically treated CT26 tumors (data not shown). Because PDT + IT-DC was effective as a treatment for both tumors, it seems likely that a relatively small number of dead or dying tumor cells can provide the necessary antigens required for DC-mediated induction of antitumor immunity. Furthermore, because it is known that PDT stimulates the expression of inflammatory cytokines such as tumor necrosis factor α, IL-1, and IL-6 (12, 13), perhaps the presence of such factors in the tumor microenvironment played a critical role in the induction of DC maturation.

In summary, the data presented in this report indicate that PDT + IT-DC results in potent systemic antitumor immunity and regression of tumors including tumors at sites distant from the treated site. Based on these findings, this novel regimen may prove beneficial in the treatment of patients with advanced metastatic disease as well as in the neoadjuvant setting before resection of tumors known to have a high recurrence rate.

Acknowledgments

We thank Claudia Benike, Linda Wu, and Ines Mende for critically reviewing the manuscript.

References

1. Hsu FJ, Benike C, Fagnoni F, et al. Vaccination of patients with B-cell lymphoma using autologous antigen pulsed dendritic cells. Nat Med 1996;2:52–8.
2. Steinman RM, Pope M. Exploiting dendritic cells to improve vaccine efficacy. J Clin Invest 2002;109:1519–26.
3. Banchereau J, Palucka K. Dendritic cells as therapeutic vaccines against cancer. Nat Rev Immunol 2005;5:296–306.
4. Fields RC, Shimizu K, Mule JJ. Murine dendritic cells pulsed with whole tumor lysates mediate potent antitumor immune responses *in vitro* and *in vivo*. Proc Natl Acad Sci U S A 1998;95:9482–7.
5. Song W, Kong HL, Carpenter H, et al. Dendritic cells genetically modified with an adenovirus vector encoding the cDNA for a model antigen induce protective and therapeutic antitumor immunity. J Exp Med 1997;186:1247–56.
6. Boczkowski D, Nair SK, Snyder D, Gilboa E. Dendritic cells pulsed with RNA are potent antigen-presenting cells *in vitro* and *in vivo*. J Exp Med 1996;184:465–72.
7. Condon C, Watkins SC, Celluzzi CM, Thompson K, Falo LD, Jr. DNA-based immunization by *in vivo* transfection of dendritic cells. Nat Med 1996;2:1122–8.
8. Gong J, Chen D, Kashiwaba M, Kufe D. Induction of antitumor activity by immunization with fusions of dendritic and carcinoma cells. Nat Med 1997;3:558–61.
9. Fong L, Engleman EG. Dendritic cells in cancer immunotherapy. Annu Rev Immunol 2000;18:245–73.
10. Engleman EG. Dendritic cell-based cancer immunotherapy. Semin Oncol 2003;30:23–9.
11. Figdor CG, De Vries JM, Lesterhuis WJ, Melief CJM. Dendritic cell immunotherapy: mapping the way. Nat Med 2004;10:475–80.
12. Dougherty TJ, Gomer CJ, Henderson BW, et al. Photodynamic therapy. J Natl Cancer Inst 1998;90:889–905.
13. Gollnick SO, Liu X, Owczarczak B, Musser DA, Henderson BW. Altered expression of interleukin 6 and interleukin 10 as a result of photodynamic therapy *in vivo*. Cancer Res 1997;57:3904–9.
14. Engleman EG, Brody J, Soares L. Using signaling pathways to overcome immune tolerance to tumors. Sci STKE 2004; pe28.
15. Furumoto K, Soares L, Engleman EG, Merad M. Induction of potent antitumor immunity by *in situ* targeting of intratumoral DCs. J Clin Invest 2004;113:774–83.
16. Mori M, Sakata I, Hirano T, et al. Photodynamic therapy for experimental tumors using ATX-S10(Na), a hydrophilic chlorin photosensitizer, and diode laser. Jpn J Cancer Res 2000;91:753–9.
17. Biel MA. Photodynamic therapy and the treatment of head and neck cancers. J Clin Laser Med Surg 1996;14:239–44.
18. Aruga A, Aruga E, Tanigawa K, Bishop DK, Sondak VK, Chang AE. Type 1 versus type 2 cytokine release by Vβ T cell subpopulations determines *in vivo* antitumor reactivity: IL-10 mediates a suppressive role. J Immunol 1997;159:664–73.
19. Barth RJ, Jr., Mule JJ, Spiess PJ, Rosenberg SA. Interferon γ and tumor necrosis factor have a role in tumor regressions mediated by murine CD8+ tumor-infiltrating lymphocytes. J Exp Med 1991;173:647–58.
20. Tong Y, Song W, Crystal RG. Combined intratumoral injection of bone marrow-derived dendritic cells and systemic chemotherapy to treat pre-existing murine tumors. Cancer Res 2001;61:7530–5.
21. Tanaka F, Yamaguchi H, Ohta M, et al. Intratumoral injection of dendritic cells after treatment of anticancer drugs induces tumor-specific antitumor effect *in vivo*. Int J Cancer 2002;101:265–9.
22. Yu B, Kusmartsev S, Cheng F, et al. Effective combination of chemotherapy and dendritic cell administration for the treatment of advanced-stage experimental breast cancer. Clin Cancer Res 2003;9:285–94.
23. Shin JY, Lee SK, Kang CD, et al. Antitumor effect of intratumoral administration of dendritic cell combination with vincristine chemotherapy in a murine fibrosarcoma model. Histol Histopathol 2003;18:435–47.
24. Teitz-Tennenbaum S, Li Q, Rynkiewicz S, et al. Radiotherapy potentiates the therapeutic efficacy of intratumoral dendritic cell administration. Cancer Res 2003;63:8466–75.
25. Ehtesham M, Kabos P, Gutierrez MA, Samoto K, Black KL, Yu JS. Intratumoral dendritic cell vaccination elicits potent tumoricidal immunity against malignant glioma in rats. J Immunother 2003;26:107–16.
26. Song W, Levy R. Therapeutic vaccination against murine lymphoma by intratumoral injection of naive dendritic cells. Cancer Res 2005;65:5958–64.
27. Gollnick SO, Vaughan L, Henderson BW. Generation of effective antitumor vaccines using photodynamic therapy. Cancer Res 2002;62:1604–8.
28. Jalili A, Makowski M, Switaj T, et al. Effective photoimmunotherapy of murine colon carcinoma induced by the combination of photodynamic therapy and dendritic cells. Clin Cancer Res 2004;10:4498–508.
29. Schoenfeld N, Mamet R, Nordenberg Y, Shafran M, Babushkin T, Malik Z. Protoporphyrin biosynthesis in melanoma B16 cells stimulated by 5-aminolevulinic acid and chemical inducers: characterization of photodynamic inactivation. Int J Cancer 1994;56:106–12.
30. Albert ML, Sauter B, Bhardwaj N. Dendritic cells acquire antigen from apoptotic cells and induce class I-restricted CTLs. Nature 1998;392:86–9.
31. Steinman RM, Turley S, Mellman I, Inaba K. The induction of tolerance by dendritic cells that have captured apoptotic cells. J Exp Med 2000;191:411–6.
32. Sauter B, Albert ML, Francisco L, Larsson M, Somersan S, Bhardwaj N. Consequences of cell death: exposure to necrotic tumor cells, but not primary tissue cells or apoptotic cells, induces the maturation of immunostimulatory dendritic cells. J Exp Med 2000;191:423–34.
33. Gallucci S, Lolkema M, Matzinger P. Natural adjuvants: endogenous activators of dendritic cells. Nat Med 1999;5:1249–55.
34. Rovere P, Vallinoto C, Bondanza A, et al. Bystander apoptosis triggers dendritic cell maturation and antigen-presenting function. J Immunol 1998;161:4467–71.

Immunohistochemical Differential Diagnosis Between Large Cell Neuroendocrine Carcinoma and Small Cell Carcinoma by Tissue Microarray Analysis With a Large Antibody Panel

Jun-ichi Nitadori, MD,[1,2,4] Genichiro Ishii, MD,[1] Koji Tsuta, MD,[1] Tomoyuki Yokose, MD,[1] Yukinori Murata, MT,[1] Tetsuro Kodama, MD,[3] Kanji Nagai, MD,[2] Harubumi Kato, MD,[4] and Atsushi Ochiai, MD[1]

Key Words: Lung cancer; Large cell neuroendocrine carcinoma; Small cell carcinoma; Tissue microarray; Immunohistochemistry; Large antibody panel

DOI: 10.1309/DT6BJ698LDX2NGGX

Abstract

To elucidate additional phenotypic differences between large cell neuroendocrine carcinoma (LCNEC) and small cell lung carcinoma (SCLC), we performed tissue microarray (TMA) analysis of surgically resected LCNEC and SCLC specimens. Immunostaining with 48 antibodies was scored based on staining intensity and the percentage of cells that stained positively. Four proteins were identified as significantly expressed in LCNEC as compared with SCLC: cytokeratin (CK)7, 113 vs 49 (P < .0301); CK18, 171 vs 60 (P < .0008); E-cadherin, 77 vs 9 (P < .0073); and β-catenin, 191 vs 120 (P < .0286). Immunostaining of cross-sections containing LCNEC and SCLC components revealed significant expression of CK7, CK18, and β-catenin in the LCNEC component compared with the SCLC component in 2 of 3 cases. Our results indicate that significant expression of CK7, CK18, E-cadherin, and β-catenin is more characteristic of LCNEC than of SCLC, and these findings provide further support that these tumor types are separate entities morphologically and immunophenotypically, if not biologically.

Lung cancer is a major cancer throughout the world and the most common cause of cancer mortality. The revised World Health Organization (WHO) classification of lung cancer published in 1999 classifies neuroendocrine tumors into 4 major histologic categories: low-grade malignant "typical" carcinoid, intermediate-grade malignant "atypical" carcinoid, and 2 high-grade tumors, large cell neuroendocrine carcinoma (LCNEC) and small cell lung carcinoma (SCLC).[1] In 1991, Travis et al[2] introduced the term *large cell neuroendocrine carcinoma* to describe a distinct category of high-grade neuroendocrine tumor with biologic and light microscopic characteristics different from those of high-grade SCLC. Morphologically, LCNEC is characterized by neuroendocrine morphologic features (rosette formation), large tumor cells (3 times larger in diameter than a small resting lymphocyte) with a low nuclear/cytoplasmic ratio, numerous nucleoli, a high mitotic rate (>10 in 10 high-power fields), a large degree of necrosis, and immunohistochemically staining positive for one or more neuroendocrine markers.

Some authors have reported that LCNEC has a poorer prognosis than SCLC,[3,4] whereas others have reported finding no significant difference in outcome between LCNEC and SCLC.[5-7] SCLC is sensitive to chemotherapy, but the optimal therapy for LCNEC has yet to be defined. Demetri et al[8] advocated that LCNEC be treated in a manner similar to SCLC but acknowledged that there may be a greater role for surgical resection in LCNEC. Nevertheless, it remains unclear how patients with LCNEC should be treated. Until now, few investigators have attempted to identify differences in molecular expression between LCNEC and SCLC. Sturm et al[9] reported a significantly higher frequency of thyroid transcription factor (TTF)-1 positivity with SCLCs, but no other biologic markers

with significantly different expression between LCNEC and SCLC have been reported.

Tissue microarray (TMA) analysis is becoming broadly accepted as an efficient and expeditious method in the field of proteomics,[10-12] and it provides a great deal of information that is equivalent to the information obtained from many tissue sections obtained from a large number of patients. It also is suitable for high-throughput molecular profiling of tumor specimens. In the present study, we used TMA with a large panel of antibodies to identify the phenotypic differences between LCNEC and SCLC.

Materials and Methods

Case Selection

During the period from January 1992 to December 2003, a total of 1,921 patients with primary lung carcinoma were treated at the National Cancer Center Hospital East, Chiba, Japan. All primary lung cancers with a pathologic diagnosis based on the classification schema of the third edition of the WHO classification[1] were reviewed, and 49 cases were diagnosed as LCNEC (2.6%). The 10 cases for which an adequate tissue specimen was not available for pathologic review were excluded from the study, leaving a total of 39 cases (2.0%) of LCNEC. TMA also was performed on specimens from 14 cases histologically diagnosed as pure SCLC (0.7%). In addition, 3 cases of SCLC combined with LCNEC were used to verify the results obtained by TMA.

Pathologic Studies

The specimens were fixed with 10% formalin and embedded in paraffin. Serial 4-μm sections were stained with H&E by the alcian blue–periodic acid–Schiff method for cytoplasmic mucin production and by the elastic van Gieson method for elastic fibers. Sections were reviewed by 3 pulmonary pathologists (J.N., G.I., and T.Y.) according to the histologic criteria described in the WHO classification criteria, and discrepancies were resolved by joint discussion of the slides viewed with a multiheaded microscope.

Construction of Tumor TMAs

The most representative tumor areas were selected carefully and marked on the H&E-stained slide for construction of microarrays. TMAs were assembled with a tissue-arraying instrument (Beecher Instruments, Silver Spring, MD).[10] The microarray system consists of thin-walled stainless steel needles approximately 2 mm in diameter and a stylet for transferring and removing the contents of the needle. The assembly is held in an x-y position guide that is manually adjusted with digital micrometers. Core samples are retrieved from selected regions of donor tissue and precisely arrayed in a new (recipient) paraffin block. Extra samples of the specimens were obtained routinely by collecting 2 replicate core samples of tumor in different areas. Specimens from the 39 cases of LCNEC **Image 1B** and **Image 1D** and 14 cases of SCLC **Image 1C** and **Image 1E** were punched, and core samples were mounted in the same donor blocks **Image 1A**.

Normal Control TMA

The normal control TMA was used as the positive control array for each staining. This slide was composed of esophagus, stomach, small intestine, large intestine, liver, pancreas, spleen, brain, heart, lung, skin, testis, kidney, prostate gland, breast, thyroid gland, and adrenal gland samples.

Antibodies and Immunohistochemical Staining

The 48 antibodies used in the study are listed in **Table 1**. Immunohistochemical staining was performed as follows: TMA donor blocks were cut into 4-μm sections and mounted on silane-coated slides. The sections were deparaffinized in xylene and dehydrated in a graded alcohol series, and endogenous peroxidase was blocked with 3% hydrogen peroxide in absolute methyl alcohol. Heat-induced epitope retrieval was performed for 20 minutes at 95°C with a 0.02-mol/L concentration of citrate buffer (pH 6.0). After the slides cooled at room temperature for 60 minutes, they were rinsed with deionized water and incubated overnight with primary antibodies. The slides then were washed 3 times with phosphate-buffered saline and incubated with the EnVision+ System-HRP (DAKO, Glostrup, Denmark). The reaction products were stained with diaminobenzidine and counterstained with hematoxylin. Some antibodies (Table 1) were used in an automated immunostainer (Ventana Medical Systems, Tucson, AZ) after antigen retrieval by microwave heating and citrate buffer.[13]

Identification of Positive Cases

The cases were evaluated in random order without knowledge of patient history. Each case in which more than 10% of the cancer cells reacted positively for an antibody were recorded as positive.

Calculation of Staining Scores

Immunostaining was scored based on the intensity of staining and the percentage of cells that stained positively. Whenever there was a disagreement, the slides were reviewed, and consensus was reached. Staining scores were calculated by multiplying the percentage of positive tumor cells per section (0% to 100%) by the immunohistochemical staining intensity. The sections were classified according to staining intensity as negative (total absence of staining), 1+ (weak staining), 2+ (moderate staining), or 3+ (strong staining), and the scores obtained ranged from 0 to 300. The staining scores obtained for 2 samples from the same specimen were calculated, and the result was recorded as the

DOI: 10.1309/DT6BJ698LDX2NGGX

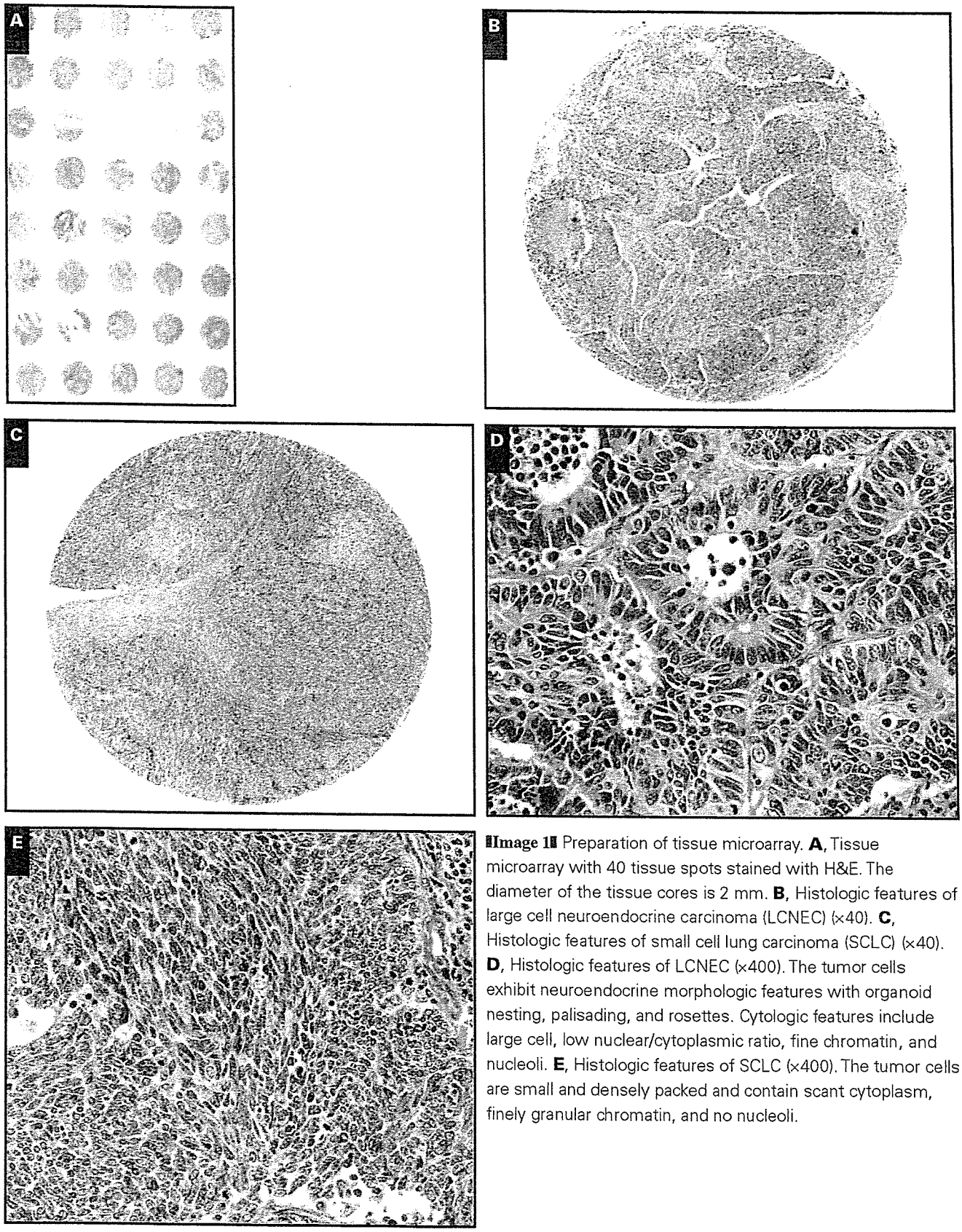

Image 1 Preparation of tissue microarray. **A**, Tissue microarray with 40 tissue spots stained with H&E. The diameter of the tissue cores is 2 mm. **B**, Histologic features of large cell neuroendocrine carcinoma (LCNEC) (×40). **C**, Histologic features of small cell lung carcinoma (SCLC) (×40). **D**, Histologic features of LCNEC (×400). The tumor cells exhibit neuroendocrine morphologic features with organoid nesting, palisading, and rosettes. Cytologic features include large cell, low nuclear/cytoplasmic ratio, fine chromatin, and nucleoli. **E**, Histologic features of SCLC (×400). The tumor cells are small and densely packed and contain scant cytoplasm, finely granular chromatin, and no nucleoli.

DOI: 10.1309/DT6BJ698LDX2NGGX

Table 1
Antibodies Used

Classification/Antibody	Clone	Pretreatment	Dilution	Source
Cytokeratins				
CK1	34βB4	Microwave	1:20	Novocastra, Newcastle upon Tyne, England
CK4	6B10	Microwave	1:100	Novocastra
CK5/6	D5/16 B4	Microwave	1:50	DakoCytomation, Carpinteria, CA
CK7	OV-TL 12/30	Microwave	1:50	DakoCytomation
CK8	35βH11	Microwave	1:25	DakoCytomation
CK10	DE-K10	Microwave	1:50	DakoCytomation
CK13	KS-1A3	Microwave	1:100	Novocastra
CK14	LL002	Microwave	1:20	Novocastra
CK15	LHK15	Microwave	1:40	Novocastra
CK17	E3	Microwave	1:20	DakoCytomation
CK18	DC10	Microwave	1:25	DakoCytomation
CK19	RCK108	Microwave	1:50	DakoCytomation
CK20	Ks20.8	Microwave	1:25	DakoCytomation
Cytoskeletal filaments and markers				
Desmin	DE-R-11	Microwave	Prediluted	Ventana Medical Systems, Tucson, AZ
S-100	Polyclonal	None	Prediluted	Ventana Medical Systems
EMA	Mc5	None	Prediluted	Ventana Medical Systems
Vimentin	3B4	Microwave	Prediluted	Ventana Medical Systems
Drug resistant gene products and related markers				
Pgp	JSB-1	Microwave	1:20	Novocastra
MRP-1	MRPm6	Microwave	1:50	Sanbio, Uden, the Netherlands
MRP-2	M2III-6	Microwave	1:20	Sanbio
BCRP	BXP21	Microwave	1:20	Sanbio
Cox-1	Polyclonal	Microwave	1:50	IBL, Gunma, Japan
Cox-2	Polyclonal	Microwave	1:50	IBL
Apoptosis-associated proteins				
bcl-2	124	Microwave	1:40	DakoCytomation
bcl-x	Polyclonal	Microwave	1:500	Becton Dickinson Biosciences, San Jose, CA
bax	Polyclonal	Microwave	1:20	Oncogene Research Products, Cambridge, MA
bcl-1	P2D11F11	Microwave	Prediluted	Ventana Medical Systems
p 53	DO-7	Microwave	1:50	DakoCytomation
Growth factors and hormone receptors				
EGFR	EGFR.113	Microwave	1:10	Novocastra
c-erbB-2	CB11	Microwave	Prediluted	Ventana Medical Systems
IGFR	24-31	Microwave	1:100	Chemicon, Temecula, CA
c-kit	Polyclonal	Microwave	1:50	DakoCytomation
PgR	1A6	Microwave	Prediluted	Ventana Medical Systems
ER	6F11	Microwave	Prediluted	Ventana Medical Systems
Cellular adhesion molecules				
β-catenin	14	Microwave	1:200	Becton Dickinson Biosciences
E-cadherin	36	Microwave	1:100	Becton Dickinson Biosciences
NCAM	NCC-Lu-243	Microwave	1:25	Nippon Kayaku, Tokyo, Japan
CD29	7F10	Microwave	1:20	Novocastra
CD44	DF1485	Microwave	1:40	Novocastra
Cluster differential markers				
CD15	BY87	Microwave	Prediluted	Ventana Medical Systems
CD30	1G12	Microwave	Prediluted	Ventana Medical Systems
Mucin-related proteins				
Muc-1	Ma695	Microwave	1:100	Novocastra
Muc-2	Ccp58	Microwave	1:100	Novocastra
Muc-5AC	CLH2	Microwave	1:50	Novocastra
Muc-6	CLH5	Microwave	1:50	Novocastra
M-CCMC-1	HIK1083	Microwave	1:10	Kanto Chemical, Tokyo, Japan
Pneumocyte differential markers				
TTF-1	8G7G3/1	Microwave	1:50	DakoCytomation
SPPB	19H7	Microwave	1:25	Novocastra

BCRP, breast cancer resistance protein; EGFR, epidermal growth factor receptor; EMA, epithelial membrane antigen; ER, estrogen receptor; IGFR, insulin-like growth factor receptor; MRP, multidrug resistance protein; NCAM, neural cell adhesion molecule; PgP, P-glycoprotein; PgR, progesterone receptor; SPPB, surfactant precursor protein B; TTF, thyroid transcription factor.

score for that case. If one sample was lost, the staining score was calculated from the data for the remaining specimen alone. The staining scores for the specimens that contained SCLC combined with LCNEC were calculated using the intensity of staining and the percentage of each component stained on the entire slide.

Statistical Analysis

The staining score data are reported as means plus 95% confidence intervals. The Mann-Whitney *U* test was used to compare the staining scores of the LCNEC group and the SCLC group. All *P* values reported are 2-sided, and the significance

DOI: 10.1309/DT6BJ698LDX2NGGX

level was set at less than .05. Differences between proportions were evaluated by using the Fisher exact test. All analyses were performed using Statview software (version 5.0 for Windows, SAS Institute, Cary, NC).

Results

Of the 5,406 core samples, 70 (1.3%) were lost on the TMA during processing of the slides for H&E preparation and immunostaining.

Positive Rates of LCNEC and SCLC

The percentages of LCNEC cases and SCLC cases that reacted positively for each antibody are summarized in **Table 2**. A positive reaction for cytokeratin (CK)18 was observed in 38 (97%) of 39 cases of LCNEC and 10 (71%) of 14 cases of SCLC, and the difference was significant ($P = .0143$). A positive reaction for E-cadherin was observed in 30 (77%) of 39 cases of LCNEC and 6 (43%) of 14 cases of SCLC, and the difference was significant ($P = .0419$).

Staining Scores for LCNEC and SCLC

The LCNEC and SCLC staining scores for each antibody are summarized in Table 2. Of the 13 cytokeratins tested, CK7 and CK18 had significantly higher staining scores in LCNEC. CK7 immunoreactivity was found in 30 (77%) of 39 cases of LCNEC and 7 (50%) of 14 cases of SCLC. The average staining score was 113 in LCNEC and 49 in SCLC; the difference was significant ($P = .0301$). **Image 2A** shows CK7 immunostaining of an LCNEC case with a staining score of 270. **Image 2B** shows CK7 immunostaining of an SCLC case with a staining score of 10. The average CK18 staining score was 171 in LCNEC and 60 in SCLC, and the difference was significant ($P = .0008$). **Image 2C** and **Image 2D** show CK18 immunostaining of an LCNEC case with a staining score of 240 and an SCLC case with a staining score of 40. No significant differences between LCNEC and SCLC were found in the expression of the other cytokeratins tested.

LCNEC had significantly higher staining scores for E-cadherin and β-catenin. E-cadherin expression was localized mainly on the membranes of the tumor cells. In some cases, E-cadherin expression was localized in the cytoplasm and nucleus, but results were recorded as negative. The average staining score for E-cadherin was 77 in LCNEC and 9 in SCLC. **Image 2E** and **Image 2F** show that the E-cadherin staining score was 80 in LCNEC and 10 in SCLC. Image 2F shows an E-cadherin staining score of 10 in SCLC. The expression of β-catenin was localized on the membranes and, in some cases, on the nucleus of the tumor cells. We classified the pattern of expression of β-catenin according to whether there was membranous or nuclear staining. Membranous β-catenin staining was found in 38 (97%) of 39 LCNEC cases and all 14 SCLC cases (100%). The average membranous β-catenin staining score was 191 in LCNEC and 120 in SCLC. **Image 2G** shows a membranous β-catenin staining score of 200 in LCNEC. **Image 2H** shows that the β-catenin staining score was 60 in SCLC. Nuclear β-catenin immunoreactivity was found in 5 (13%) of 39 LCNEC cases but in 0 (0%) of 14 SCLC cases. The average nuclear β-catenin staining score was 31 in LCNEC and 0 in SCLC, and the difference was not significant ($P = .4801$). There were no significant differences between LCNEC and SCLC in expression of the other cellular adhesion molecules.

We evaluated the expression of several other biologic markers, but no differences in expression were found between LCNEC and SCLC (Table 2).

Immunohistochemical Staining of CK7, CK18, E-Cadherin, and β-Catenin in Cross-Sections Containing LCNEC and SCLC Components

To determine whether the differences in expression of CK7, CK18, E-cadherin, and β-catenin in LCNEC and SCLC found as a result of the TMA analysis could be applied generally, their expression was evaluated in 3 cases of combined SCLC and LCNEC on slides that contained both components. The staining scores in these 3 cases are summarized in **Table 3**. In cases 1 and 2, expression of CK7, CK18, and β-catenin was clearly higher in the LCNEC components **Image 3**, and the results for these antibodies seemed similar to the results of TMA; however, E-cadherin expression was modestly higher in the LCNEC component in 1 case (case 1).

Discussion

The aim of the present study was to identify the distinct immunophenotypes of LCNEC and SCLC, and the technique used was based on large-scale analysis of protein expression detected by immunohistochemical analysis. Although it must be kept in mind that a potential limitation of TMA is that small core samples might not be representative of whole tumors, particularly in heterogeneous cancers,[14] the use of TMA has the advantage of enabling protein profiling, which probably more closely reflects the biologic characteristics of the tumor cells than does RNA detection. In the present study, we used the products of the staining intensity and distribution scores to assess immunoreactivity because they reveal phenotypic differences in greater detail. The TMA method identified 4 proteins as being overexpressed in LCNEC compared with SCLC: CK7 and CK18, which are involved in cytoskeleton organization, and β-catenin and E-cadherin, which are involved in cell adhesion. The results obtained were not surprising because the most striking morphologic differences between LCNEC and SCLC are cell shape and adhesiveness.

DOI: 10.1309/DT6BJ698LDX2NGGX